Restricted Segmental Mobility in Side-Chain Crystalline Comblike Polymers, Studied by Dielectric Relaxation Measurements

I. Alig,* M. Jarek, and G. P. Hellmann

Deutsches Kunststoff-Institut, Schlossgartenstrasse 6, D-64289 Darmstadt, Germany

Received August 21, 1997; Revised Manuscript Received November 13, 1997

ABSTRACT: The dynamics of comblike polymers with a methacrylic backbone and flexible side chains were investigated by frequency and temperature dependent dielectric measurements. The cooperative motions of the main-chain segments and the side chains were first characterized in an amorphous polymer, i.e., the homopolymer of oleoyl methacrylate (POMA). Then the chemically similar homopolymers of stearyl (PSMA) and perfluorododecyl methacrylate (PFMA) were studied where the side chains can crystallize, forming lamellae. Above the melting point, the segmental relaxations of PSMA and PFMA are similar to those of the amorphous POMA. Below the melting point, however, the mobility of the methacrylic main chains is almost entirely suppressed, although the chain backbones are not built into the crystalline lamellae of the side chains. As a particularly interesting case, the random copolymer (SMA−FMA) of stearyl (SMA) and perfluorododecyl (FMA) methacrylate units in equal shares was studied. In SMA−FMA, the SMA and FMA side chains crystallize independently in a bilayer structure. The FMA side chains melt at a higher temperature than the SMA side chains. Between the two melting points, the copolymer SMA−FMA consists alternatingly of molten SMA lamellae and crystalline FMA lamellae. In this situation, the methacrylic main chains are expected to be only partly liberated. In fact, the relaxation strength was found to increase stepwise at the melting points but also continuously between the melting points. The latter phenomenon indicates that, in the restricted bilayer structure of a comblike copolymer where molten and crystalline side-chain layers alternate, the crystalline layers lose, at increasing temperatures, successively their immobilizing effect on the main chain.

I. Introduction

Most atactic vinyl polymers are amorphous: Their monomer sequences are too irregular to arrange in an ordered array of crystalline chain segments. In comblike polymers,[1−6] however, atactic chains can indirectly be forced into crystals. This paper deals with the molecular mobility, in different amorphous and crystalline states, of comblike polymers, as indicated schematically in Figure 1 with an atactic main chain and linear branches ("side chains"), both conformationally flexible. At high temperatures, such comblike chains form random coils (Figure 1a). But if long and regular enough, the branches can crystallize above room temperature in lamellae (Figure 1b) that force the polymer backbones into ordered double-comb conformations (Figure 1c). The backbones are forced to form quasi-amorphous interlayers between the crystalline side-chain lamellae. The squeezed-in polymer main chains are probably straightened out over relatively long sequences and cross sometimes through the lamellae (Figure 1d). The chain backbones of comblike polymers are thus not really incorporated in the crystalline order of the side chains but are nonetheless part of the total crystal.

In the following report, the consequences of this situation of squeezed-in polymer chains on the mobility of the chain segments are discussed in homopolymers with only one type of side chains and in copolymers with two different types of side chain.

The segmental motions were probed by temperature and frequency dependent dielectric relaxation measurements. Dielectric spectroscopy has been applied for a long time to characterize the relaxation behavior of polymers but most attention has been devoted to amorphous polymers and not to semicrystalline polymers and their thermal transitions.[7] However, dielectric spectroscopy is also a very useful technique to study the restrictions that are imposed on the conformations and motions of polymer segments by crystallization.[8] Side-chain crystallizing comblike polymers are particularly interesting objects, due to their special architecture: every monomer unit of the chains is both crystalline (in the branch) and amorphous (in the backbone).

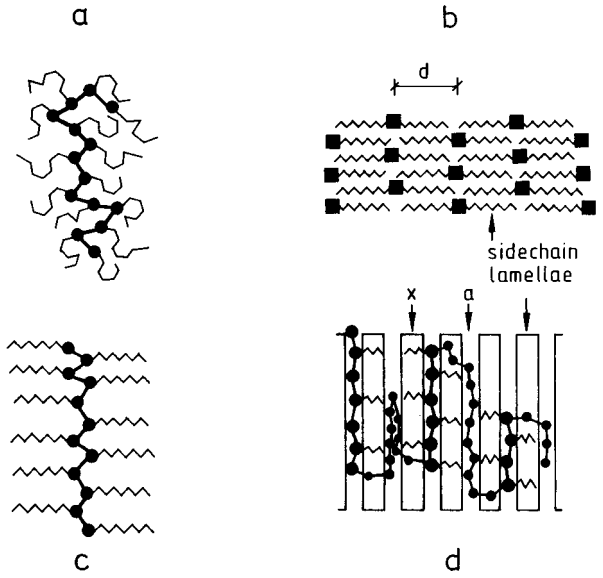

Figure 1. Structure of a comblike polymer with flexible side chains: (a) coil conformation in the melt and (b)−(d) layer structures, ordered due to side-chain crystallization, (b) lamellar structure (■, main chains, perpendicular to the paper; *d*, long period), (c) double-comb conformation, (d) top view of the structure of (b) (x, crystalline; a, amorphous).

* To whom the correspondence should be addressed.

S0024-9297(97)01261-8 CCC: $15.00
Published on Web 03/15/1998

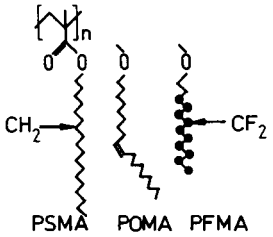

Figure 2. Homopolymers with a methacrylic main chain ($n \cong 10^2$: degree of polymerization), substituted with stearyl (PSMA), oleoyl (POMA). or 1*H*,1*H*,2*H*,2*H*-perfluorododecyl side chains (PFMA).

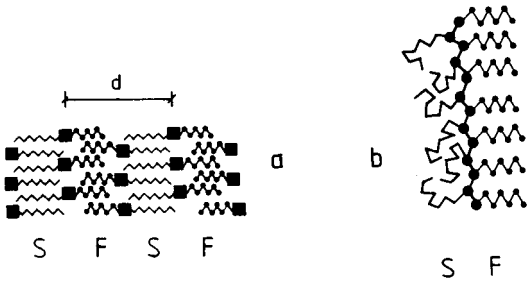

Figure 3. (a) Bilayer structure of the copolymer SMA−FMA with stearyl (S) and perfluorododecyl (F) side chains layers (■, main chains), long period *d*. (b) Bilayer chain conformation of SMA−FMA at temperatures between the melting points. The stearyl (S) branches are molten and flexible, while the perfluorododecyl (F) branches are crystalline and immobilized.

This intimate contact of crystalline order and amorphous disorder is unique.

This report has two parts. In the first, the dynamics of two chemically very similar polymers, i.e., of polystearyl (PSMA)[1] and polyoleoyl (POMA) methacrylate, are compared (Figure 2). The stearyl branches of PSMA can crystallize, whereas the oleoyl branches of POMA cannot, due to a cis double bond in the alkyl sequence. PSMA and POMA are well suited for dielectric measurements, inasmuch as the electric field couples mainly with the COO ester dipole, which is placed in a strategic position, at the junction of the main and the side chains. The dipole moment of the side chains can be almost neglected.

In the second part of this report, the discussion is extended to a polymer of fluorinated dodecyl methacrylate (PFMA, Figure 2)[9,10] and a random 1:1 copolymer (SMA−FMA) of SMA and FMA. The FMA branches crystallize with a higher melting point than the SMA branches. The copolymer SMA−FMA contains the two species of crystallizing branches, SMA and FMA, in a random sequence along the chain backbone. The SMA and FMA side chains are incompatible and, moreover, form incommensurate crystal lamellae. The SMA−FMA copolymer features two separate melting points for the SMA and FMA side chains and forms, according to X-ray data, a bilayer structure. This suggests that the SMA and FMA side chains segregate from each other along the methacrylic main chains and the copolymer crystallizes in a bilayer structure, as indicated in Figure 3a. The two layers crystallize and melt independently. Particularly interesting is the temperature range between the two melting points where the SMA layers are molten whereas the FMA layers are crystalline (Figure 3b).

The structure,[1] dynamics,[1,11] and the melting behavior[3] of comblike polymers have been investigated by several groups. Plate and Shibaev[1] discussed dielectric spectroscopy, mechanical methods, and NMR spectroscopy as tools to study the molecular mobility in comblike polymers with polyacrylate, polymethacrylate, poly(vinyl ether), and poly(vinyl ester) main chains. Early dielectric relaxation and NMR investigations by Borisova et al.[11] were related to polyhexadecyl acrylate and methacrylate, poly(vinyl stearate), and their monomers. The dielectric study was restricted to temperatures below the melting point of the side chains and thus focused on the low-temperature relaxation that is caused by local motion processes inside the side chains (frequently referred to as the γ relaxation). These processes are apparently controlled by the crystalline order. Comparison of the side-chain crystallized polymers poly(hexadecyl acrylate) and poly(hexadecyl methacrylate) revealed a stronger low-temperature relaxation in the latter, while the opposite is observed in amorphous homologues of these polymers. It was concluded that the main chain of the polyacrylate, but not that of the polymethacrylate, was involved in the crystalline order of the side chains. The segmental relaxation of the polymer backbones was not discussed.

The present report is primarily concerned with this segmental mobility of the chain backbones. Comblike homopolymers and copolymers were studied in the amorphous melt as well as in states where the side chains are crystallized. PSMA, PFMA, and SMA−FMA were chosen because the combination of apolar side chains with a moderately polar main chain makes them promising for thin-layer applications.[12−14] The main-chain dynamics are important for the mechanical performance. Briefly, the low-temperature relaxation processes inside the side chains are discussed, too.

Table 1. Temperature and Heat Effect of the Thermal Transitions and Long Period *d* of the Comblike Polymers

	transitions (°C)	heat (J/g)	period *d* (nm)
POMA	$T_g = -40$		
PSMA	$T_m \cong 45$	75	3.0
PFMA	$T_m \cong 130$	10	3.5
SMA−FMA	$T_{mSMA} = 38$	27	6.5
	$T_{mFMA} = 95$	3	

II. Experimental Section

The monomers OMA, SMA, and FMA were prepared by azeotropic esterification of the respective side-chain alcohols with methacrylic acid, catalyzed by toluenesulfonic acid, in toluene. The homopolymers POMA, PSMA, and PFMA (Figure 2) and the copolymer SMA−FMA (with equal mole fractions of SMA and FMA) were prepared by radical polymerization, using AIBN as an initiator. Tests, where the copolymerization was stopped at low conversion, confirmed that the monomers SMA and FMA are incorporated into the copolymer chains at random. The molecular weights were in the range of $M_w = 50 \times 10^3$, with a polydispersity of approximately $M_w/M_n = 3$, according to polystyrene (PS)-calibrated gel permeation chromatography (GPC).

Phase transitions were determined by differential scanning calorimetry at a heating rate of 10 K/min and polarized light microscopy. The layer structures were determined by small-angle X-ray scattering in reflection (Siemens Kristalloflex D506, Cu Kα radiation), on film samples cooled slowly from the melt (Table 1).

The dielectric relaxation spectra were measured with a HP4192 impedance analyzer in the frequency range of 1 kHz to 10 MHz. The samples were confined between two 5×20 mm^2 electrodes at a spacing of 50 ± 1 μm maintained by glass fibers. The temperature was controlled by heating against liquid nitrogen cooling, with an accuracy of ± 0.5 K.

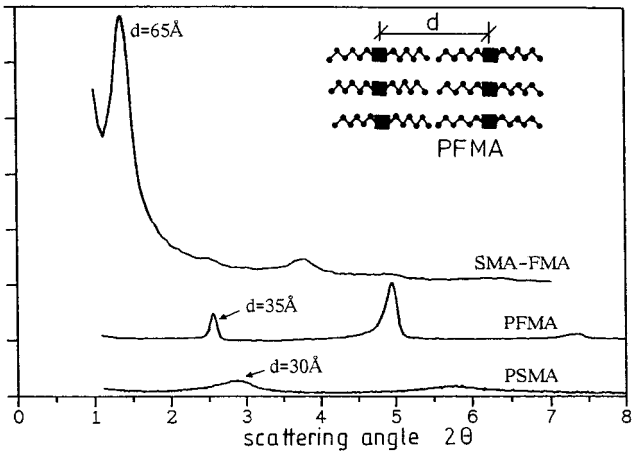

Figure 4. X-ray scattering curves. The long periods d indicate the following structures: PSMA as in Figure 1b, SMA−FMA as in Figure 3a, and PFMA as indicated in this figure.

The complex dielectric permittivity $\epsilon^*(\omega) = \epsilon'(\omega) + i\epsilon''(\omega)$ of a macroscopic system can be expressed by the one-sided Fourier transform of the time derivative of the normalized response function $\Phi(t)$ for the dielectric polarization:[15−17]

$$[\epsilon^*(\omega) - \epsilon_\infty]/\Delta\epsilon = \int_0^\infty \exp(i\omega t)[\partial\Phi/\partial t]\, dt \qquad (1)$$

where $\Delta\epsilon = \epsilon_{stat} - \epsilon_\infty$ is the relaxation strength defined by the limiting low (ϵ_{stat}) and high (ϵ_∞) frequency values of ϵ^*. The experimental data of $\epsilon^*(\omega)$ were fitted in the complex plane with the Kohlrausch−Williams−Watts (KWW) response function[17,18]

$$\Phi_{KWW}(t) = \exp[-(t/\tau)^\beta] \qquad 0 < \beta \le 1 \qquad (2)$$

where τ is the characteristic relaxation time and β describes the (asymmetric) width of the relaxation time distribution. The contribution due to conductivity in the samples at low frequencies was subtracted before data analysis. Maxwell−Wagner−Sillars polarization indicating a two-phase structure was not observed in the frequency range investigated.

III. Segmental or Main Relaxation

The glass transition and melting temperatures in Table 1 show that POMA is at room temperature a tacky elastomer whereas PSMA and PFMA are crystalline solids. The copolymer SMA−FMA features two melting points, one each for the separate SMA and FMA layers indicated in the bilayer structure in Figure 3a. Both melting points of SMA−FMA are somewhat lower than in the homopolymers PSMA and PFMA, especially T_{mFMA}. This may reflect some interlayer mixing in the copolymer or a smaller size of the crystallites.

The small-angle X-ray scattering curves of PSMA and PFMA in Figure 4 indicate two different types of structure: the long period d of PSMA equals approximately the length of one SMA branch, while that of PFMA equals the length of two FMA branches. Consequently, PSMA crystallizes as shown in Figure 1b, with a staggered zigzag arrangement of the main chains, while PFMA crystallizes with the main chains eclipsed, i.e., on top of each other, as indicated inside Figure 4.

It is important to notice that the copolymer SMA−FMA has an extra large long period, $d = 6.5$ nm, which is equal to the sum of one SMA and one FMA branch. This confirms the bilayer structure with separate SMA and FMA layers that was suggested in Figure 3a.

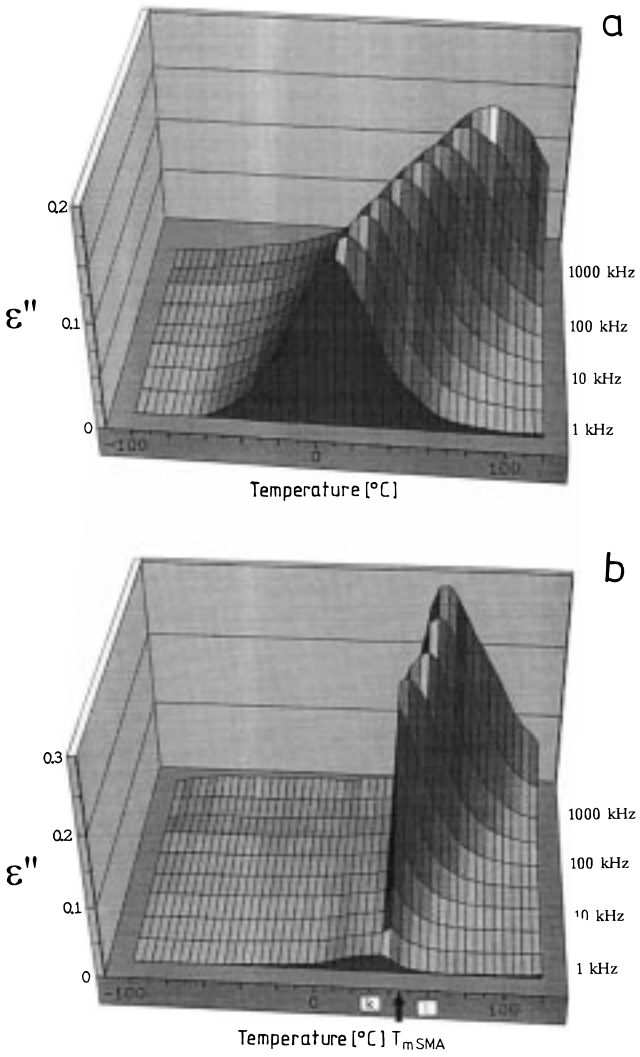

Figure 5. Temperature and frequency dependence of the dielectric loss ϵ'' for (a) POMA and (b) PSMA. T_{mSMA}: melting point of the stearyl branches (k, crystalline; i, isotropic).

POMA and PSMA. The dielectric relaxation spectra of POMA and PSMA are compared in Figure 5. The amorphous POMA exhibits a main relaxation (Figure 5a) that corresponds to the DSC glass transition (Table 1). Since the oleoyl branches of POMA and the stearyl branches of PSMA are chemically almost equal, PSMA was expected to exhibit almost the same relaxation behavior as POMA. Indeed, Figure 5b features a main relaxation of PSMA that is similar to that of POMA in Figure 5a, but *only above the melting point* T_{mSMA}. Below the melting point, on the contrary, the main relaxation is completely suppressed by the side-chain crystallization. Only a very weak low-temperature relaxation is detected (see later).

The sudden cutoff of the main relaxation below T_{mSMA} was somewhat surprising. One might have expected some residual mobility in crystalline PSMA since the stearyl branches cannot crystallize in full length (Chart 1): being chemically tied to the atactic main chain, a short "spacer" sequence of each branch must remain practically amorphous (as in smectic side-chain LC polymers). The main chains, embedded by spacers, could have retained some mobility. But Figure 5b proves otherwise: the crystalline SMA side chains immobilize the main-chain segments and spacers very efficiently.

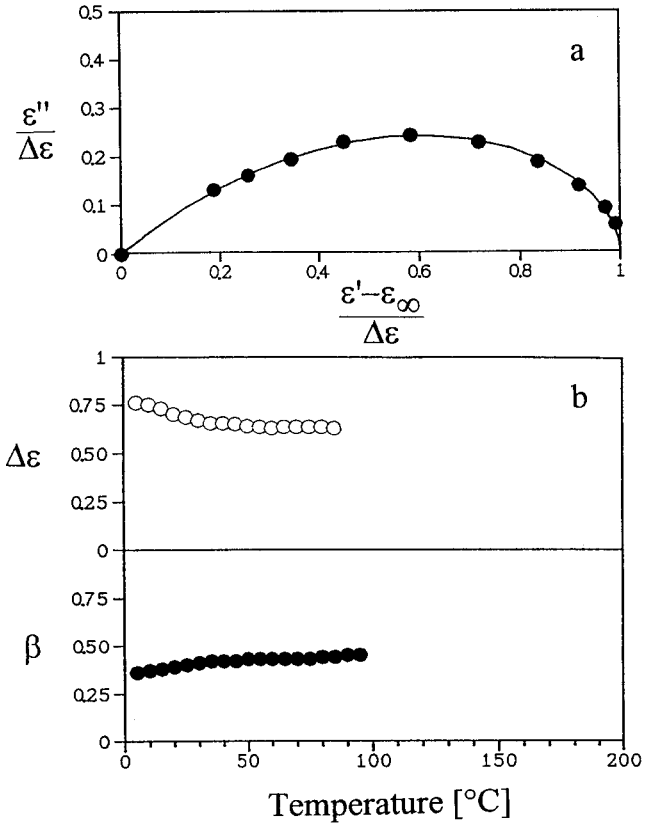

Figure 6. Relaxation behavior of POMA: (a) normalized complex−plane plot of the dielectric storage (ϵ') and loss (ϵ'') compliance (points, measured; line, calculated with eq 1 and eq 2 ($\tau = 3.6\ \mu$s, $\beta = 0.44$, $\Delta\epsilon = 0.63$, $\epsilon_\infty = 2.6$); (b) relaxation strength $\Delta\epsilon$ and KWW parameter β as functions of the temperature.

Chart 1. Methacryl Main Chain (MA) and SMA Side Chains (S), Crystalline Lamellae (k), and Amorphous Interlayer (a) Consisting of the Main Chain and Spacers

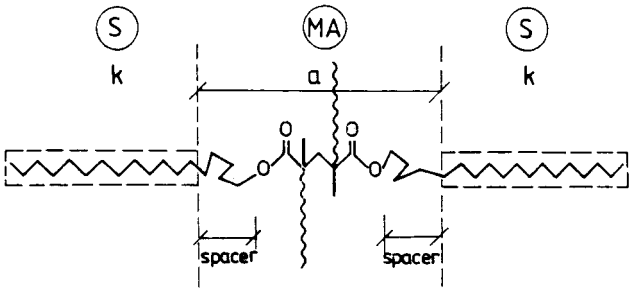

The main relaxation of POMA in Figure 5a was evaluated in detail. The normalized complex−plane plot in Figure 6a is shown as an example of the data analysis. The relaxation time τ, the distribution parameter β, and the relaxation strength $\Delta\epsilon$ were determined using eqs 1 and 2. As witnessed by Figure 6a, POMA features only one main relaxation peak. A pronounced "β" relaxation as known from poly(methyl methacrylate) (PMMA)[7,19] is not observed, in the frequency range covered. In polymethacrylates with longer side chains, the "β" relaxation is known to merge with the α relaxation.[19]

The temperature plots in Figure 6b show a decrease of the relaxation strength $\Delta\epsilon$ and an increase of the parameter β (0.35−0.48). The latter suggests that the cooperativity of the segmental motions decreases with temperature.

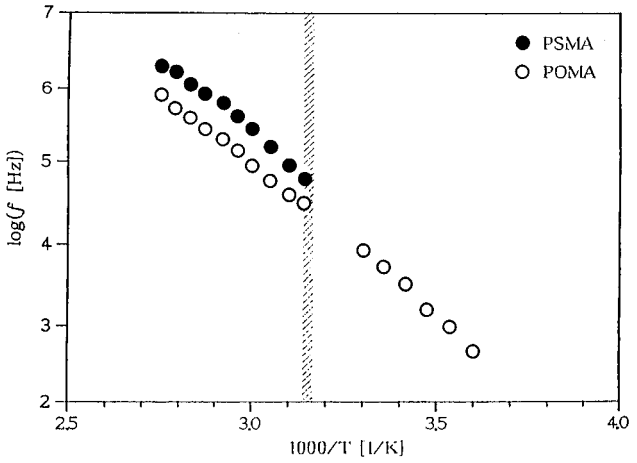

Figure 7. Arrhenius plot for the main relaxation of POMA and PSMA. The dashed vertical line indicates the melting point T_{mSMA} of PSMA (f: characteristic relaxation frequency).

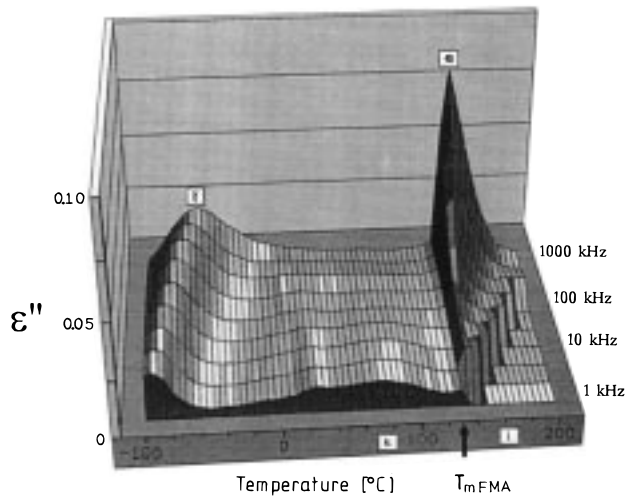

Figure 8. Temperature and frequency dependence of the dielectric loss ϵ'' of PFMA, main relaxation "α", and a low-temperature relaxation "γ". T_{mFMA}: melting point of the perfluorododecyl branches (k, crystalline; i, isotropic).

The characteristic frequencies [$f = 1/(2\pi\tau)$] are presented in Figure 7 in an Arrhenius plot. The POMA data yield a bent WLF curve rather than a straight Arrhenius line. PSMA is more difficult to judge, since the data evaluation was hampered by the cutoff at T_{mSMA} (Figure 5b). Above the melting point, the main relaxations of POMA and PSMA are very similar. The relaxation frequencies for POMA are shifted slightly to lower values (Figure 7). The difference between the two curves is small and it may be explained by the slightly higher stiffness of the POMA side chain.

PFMA and SMA−FMA. In the side-chain fluorinated homopolymer PFMA, too, crystallization of the branches suppresses the main-chain mobility, as shown in Figure 8. The main relaxation is cut off rigorously at the melting point. This prevented an exact data analysis. So an Arrhenius plot as Figure 7 could not be constructed. At very low temperatures, PFMA retains some secondary mobility (see below).

To summarize, crystalline side-chain lamellae immobilize efficiently the main chains of the comblike homopolymers PSMA and PFMA. This raises the question, how does side-chain crystallinity affect the copolymer SMA−FMA, which crystallizes in the bilayer structure as indicated in Figure 3a and melts in two

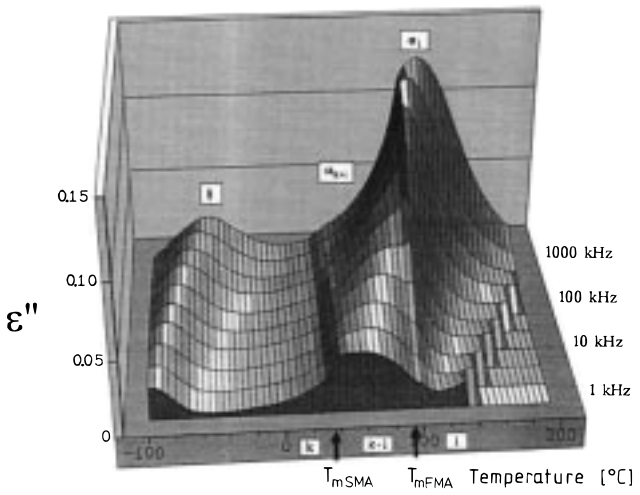

Figure 9. Temperature and frequency dependence of the dielectric loss ϵ'' of the copolymer SMA−FMA, main relaxation "α_i" (in the isotropic melt) and "α_{k+i}" (between the melting points), and a low-temperature relaxation ("γ"). T_{mSMA}, T_{mFMA}: melting points of the SMA and FMA branches (k, crystalline; i, isotropic; k + i, crystalline FMA branches and isotropic SMA branches).

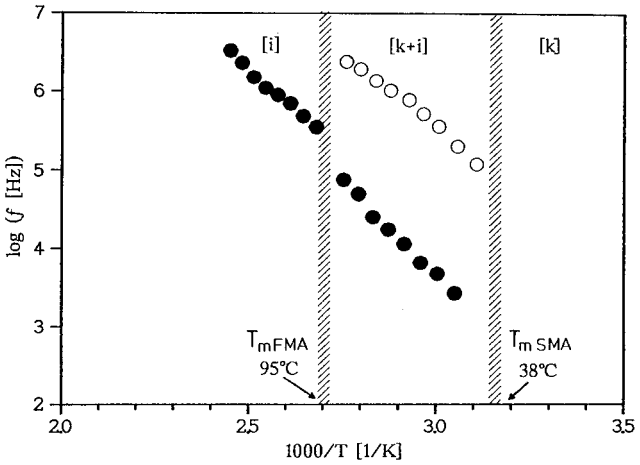

Figure 10. Arrhenius plot for SMA−FMA (full symbols) and PSMA (empty symbols, from Figure 7). the dashed vertical lines indicate the melting points.

steps, the SMA layers at T_{mSMA} = 38 °C and the FMA layers at T_{mFMA} = 95 °C (see Table 1)?

The two melting points divide the dielectric relaxation spectrum of SMA−FMA in Figure 9 into three temperature regions. Below T_{mSMA} (phase "k"), the relaxation activity is largely suppressed. Only a low-temperature relaxation (γ) is observed (see below). Above T_{mFMA}, in the isotropic melt (phase "i"), the activity of the main relaxation of SMA−FMA is developed in full strength (peak α_i). Comparison of the relaxation times in the isotropic melts of PSMA (above T_{mSMA}) and SMA−FMA (above T_{mFMA}) in Figure 10 reveals that the FMA side chains in SMA−FMA slow the segmental motions down. The segmental motions in PSMA homopolymer are faster by 1 order of magnitude.

Special about SMA−FMA is the temperature range in Figure 9 between the melting points (phase "k + i", $T_{mSMA} < T < T_{mFMA}$). The copolymer has in this range "k + i" the halfway immobilized structure indicated in Figure 3b. The SMA branches are molten, but the FMA branches, crystalline. A fairly pronounced peak ("α_{k+i}")

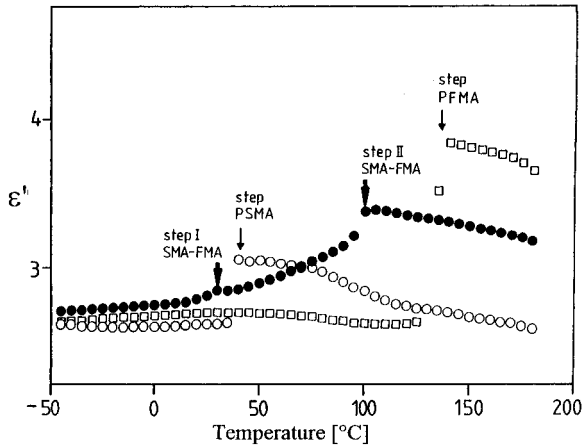

Figure 11. Dielectric constant $\epsilon'(T)$ (at f = 10 Hz) of the homopolymers PSMA and PFMA and the copolymer SMA−FMA. The arrows point to the steps at the melting points.

in Figure 9 indicates that the main relaxation is under these conditions surprisingly intense. Three effects are observed, concerning this range "k + i" of SMA−FMA between the melting points, which are illustrated by Figures 10−14.

Relaxation Times. The curve of the relaxation times of SMA−FMA in the Arrhenius plot in Figure 10 shows only a small step (factor of about two) at T_{mFMA}. The fact that the FMA branches are crystalline, below T_{mFMA}, does not seem to change the main-chain mobility much. However, a close inspection of the curve of the dielectric constant ϵ'(T) in Figure 11 reveals more details.

Relaxation Strength. The curve of the relaxation strength $\Delta\epsilon$(T) of SMA−FMA in Figure 12a, extracted from KWW fits (see above), indicates a stepwise activation of mobility at the melting points. However, due to the limited frequency range for fitting, the data the thermal activation of the main-chain mobility is better resolved in the curve of the dielectric constant $\epsilon'(T)$ at 10 kHz shown in Figure 11. PSMA, PFMA, and SMA−FMA are compared.

The segmental mobility of the homopolymers PSMA and PFMA is activated at their melting point, as indicated by a step in $\epsilon'(T)$. In the isotropic melt above the melting point, $\epsilon'(T)$ decreases monotonically in the usual fashion. For an as yet unknown reason, the step of $\epsilon'(T)$ is larger for PFMA. Since the SMA and FMA side chains are basically apolar, the steps should be almost equal.

While the relaxation strength of the homopolymers is fully activated in one single step, the behavior of the copolymer SMA−FMA is more complex: its curve $\epsilon'(T)$ exhibits two steps at the melting points T_{mSMA} and T_{mFMA}. However, $\epsilon'(T)$ is not constant between these steps but increases steadily. Above T_{mFMA}, in the isotropic state, SMA−FMA reaches its full relaxation activity at a level approximately halfway between the two homopolymers.

To emphasize an important detail, the curve of SMA−FMA in Figure 11 is repeated in Figure 13a. For comparison, a model curve is indicated with two steps and a plateau in between. This curve represents the case of total dynamic decoupling of the SMA and FMA side chains: it assumes that the SMA side chains gain their full mobility at T_{mSMA} and the FMA side chains at T_{mFMA}. But the experimental curve $\epsilon'(T)$ of SMA−FMA does not correspond to this case. The two steps

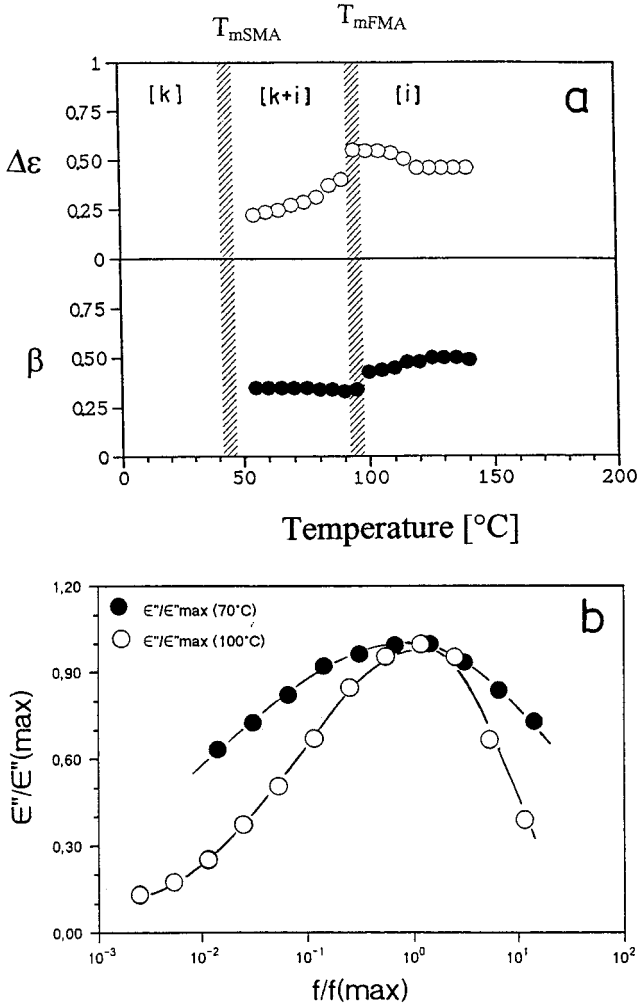

Figure 12. Relaxation strength $\Delta\epsilon$ (a) and KKW parameter β of SMA−FMA as functions of the temperature. The dashed vertical lines indicate the melting points T_{mSMA} and T_{mFMA}. (b) Normalized dielectric loss ϵ''/ϵ''(max) as a function of the normalized frequency f/f(max) of SMA−FMA at 70 °C (below T_{mFMA}) and 100 °C (above T_{mFMA}). f(max) indicates the frequency position of the maximum in ϵ'', and ϵ''(max) is the corresponding maximum value.

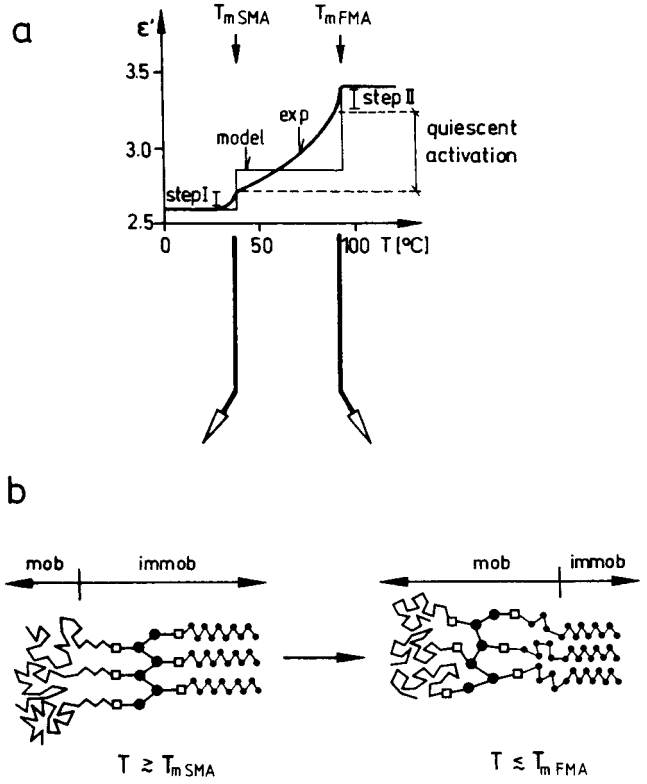

Figure 13. Mobility of the methacrylic backbone of SMA−FMA in the temperature range between the melting points T_{mSMA} and T_{mFMA}: (a) model curve with two steps and experimental curve $\epsilon'(T)$ from Figure 11 with two steps (I and II) and, between them, a steadily increasing slope; (b) main-chain mobility just above T_{mSMA} (left, most COO functions frozen-in) and just below T_{mFMA} (right, most COO functions mobile).

at the melting points T_{mSMA} and T_{mFMA} are, in fact, quite small. More than half of the mobility of SMA−FMA is activated *between, not at, the melting points*, gradually, in a process of quiescent activation.

This suggests dynamics as shown in Figure 13b. Just above T_{mSMA}, the crystalline FMA side-chain layers immobilize most COO groups, including those connected with the molten SMA side chains, so efficiently that they cannot move: the main chain is practically frozen in. But further heating increases the mobility steadily until, just below T_{mFMA}, even part of the COO groups connected with (the still crystalline) FMA side chains are mobile: the main chain is basically free to move. One may speculate that some mobility inside the crystalline FMA layers permits this increasing segmental main-chain mobility.

The side groups of PSMA and PFMA consist of $-(CH_2)-$ and $-(CF_2)-$ segments, respectively, essentially the same units as polyethylene (PE) and poly(tetrafluoroethylene) (PTFE). Both PE and PFTE have crystalline relaxations[7] that are operative below their melting points and are assumed to involve a kind of rotation/translation of chains through the crystal. Yet, no direct proof was found for this kind of crystalline relaxation for PSMA and PFMA in the frequency range considered. The different structure of semicrystalline main-chain lamellae and the crystals of short side chains may explain the absence of those relaxations.

***β* Parameter.** The β parameter in Figure 12a, extracted from KKW fits of the segmental relaxation, exhibits a step at T_{mFMA}, which indicates a change in the distribution of relaxation times. This is also reflected by the width of the ϵ'' peaks in Figure 12b below and above T_{mFMA}. The relaxation peak is broader when the FMA side chains are crystalline because the crystalline layers impose additional restrictions on the motions of the amorphous layers, which can result in a broader distribution of relaxation times. No indication for a broadening of the relaxation spectrum due to composition fluctuations[20] by intermixing of the two components above T_{mFMA} can be seen.

IV. Low-Temperature Relaxation

All polymers, POMA, PSMA, and PFMA and the copolymer SMA−FMA, feature a relaxation at very low temperatures (γ). The corresponding dielectric peaks are very weak in POMA and PSMA (Figure 5) and become apparent only in a high-resolution analysis. In PFMA and SMA−FMA (Figures 8 and 9), a larger "γ" relaxation is detected. The low-temperature position of these relaxations indicates mechanisms of local motions inside the side chains, most probably in the spacer part (Chart 1) that couples with the COO dipole. All relaxations obey an Arrhenius law with similar activa-

tion energies, 33 kJ/mol (POMA, PSMA) and 22 kJ/mol (PFMA, SMA−FMA). Borisova et al.[11] observed a somewhat higher value, 50 kJ/mol, for poly(hexadecyl methacrylate).[11] One can assume that the motion mechanisms in all these side chains are similar.

That the "γ" relaxation is in PFMA and SMA−FMA much more intense than in POMA and PSMA reflects the low interior order in the FMA side-chain crystals which, as mentioned above, melt with an uncommonly low heat. The low-temperature relaxation in the SMA−FMA copolymer is evidently directly related to that of PFMA ("γ" in Figures 8 and 9) meaning that, in the bilayer structure of SMA−FMA, the FMA side chains are internally more mobile than the SMA side chains.

V. Conclusions

Dielectric relaxation measurements proved in the present study to be very informative for investigation of the molecular mobility in systems with complex phase morphology. The investigation of the comblike homopolymers POMA, PSMA, and PFMA and the bilayer-forming comblike copolymer SMA−FMA led to the following picture.

The melting transitions of the side chains in these polymers are clearly reflected in the dielectric function, by pronounced discontinuities. The copolymer features two melting transitions.

Since only the COO dipole, which is directly attached to the main-chain segments, is dielectrically active in these polymers, the observed dielectric relaxations indicate mainly the segmental mobility of the main chains (disregarding the low-temperature relaxation). This mobility is characteristically restricted by side-chain crystallization.

Crystallization of the side chains in the homopolymers PSMA and PFMA suppresses the main relaxation processes drastically. The main chains, being squeezed between the immobilized side-chain lamellae, are unable to move on a segmental scale.

In the bilayer structure of the copolymer SMA−FMA, too, crystallization of both side chains immobilizes the main chains very efficiently. But, between the two melting points, where only the FMA side chains are crystalline while the SMA side chains are molten, the main-chain segments become mobile and the mobility increases with increasing temperature.

The last point is particularly interesting. It elucidates the dynamics of a polymer subject to *one-sided immobilization*. As indicated in Figure 3b, the polymer chains are immobilized on one side, by a crystalline (FMA) side-chain lamella, but relatively free to move on the other side, where they are attached to molten (SMA) side chains. This is a complex nanophase situation. The data show that the chains are, although squeezed into a bilayer structure, in this situation segmentally quite mobile. Systematic dielectric investigations on bilayer-forming comblike copolymers, with crystalline, liquid crystalline, and amorphous side chains layers, are in progress.

Acknowledgment. The financial support from the Deutsche Forschungsgemeinschaft (DFG, Project Al 95/2-1) is gratefully acknowledged.

References and Notes

(1) Plate, N. A.; Shibaev, V. P. *J. Polym. Sci., Macromol. Rev.* **1974**, *8*, 117.
(2) Wunderlich, B. *Macromolecular Physics*; Plenum Press: New York, 1980; Vol. 3, p 325.
(3) Jordan, E. F.; Feldeisen, D. W.; Wrigley, A. N. *J. Polym. Sci., Polym. Chem. Ed.* **1971**, *9*, 1835. Jordan, E. F.; Artymyshyn, B.; Speca, A.; Wrigley, A. N. *J. Polym. Sci., Polym. Chem. Ed.* **1971**, *8*, 3349. Jordan, E. F. *J. Polym. Sci., Polym. Chem. Ed.* **1971**, *9*, 3367.
(4) Hsieh, H. W. S.; Post, B.; Morawetz, H. *J. Polym. Sci. Phys.* **1976**, *14*, 1241.
(5) Rubin, I. D. *J. Appl. Polym. Sci.* **1988**, *36*, 445.
(6) Neumann, H. J.; Jarek, M.; Hellmann, G. P. *Macromolecules* **1993**, *26*, 2489. Braun, D.; Neumann, H. J.; Hellmann, G. P. *Makromol. Chem.* **1993**, *194*, 2349. Alig, I.; Braun, D.; Jarek, M.; Hellmann, G. P. *Macromol. Symp.* **1995**, *90*, 173.
(7) McCrum, N. G.; Read, B. E.; Williams, G. *Anelastic and Dielectric Effects in Polymer Solids*; Wiley: London, 1967.
(8) Coburn, J. C.; Boyd, H. *Macromolecules* **1986**, *19*, 2238.
(9) Kissa, E. *Fluorinated Surfactants, Synthesis-Properties-Applications*; Marcel Dekker: New York, 1984.
(10) Sheiko, S.; Lermann, E.; Möller, M. *Langmuir* **1996**, *12*, 4015.
(11) Borisova, T. I.; Burstein, L. L.; Shevelenev, V. A.; Shibaev, V. P.; Plate, N. A. *Vysokomol. Soed.* **1971**, *A13*, 2337. Borisov, T. I.; Burstein, L. L.; Malinovskaja, I. P.; Stepanova, G. P.; Plate, N. A.; Shibaev, V. P. *Vysokomol. Soed.* **1971**, *A15*, 674.
(12) Schouten, A. J.; Wegner, G. *Makromol. Chem.* **1991**, *192*, 2203. Arndt, T.; Schouten, A. J.; Schmidt, G. F.; Wegner, G. *Makromol. Chem.* **1991**, *192*, 2215.
(13) Hopken, J.; Möller, M. *Macromolecules* **1992**, *25*, 1461.
(14) Kassis, C. M.; Steehler, J. K.; Betts, D. E.; Guan, Z.; Tomack, T. J.; DeSimone, J. M.; Linton, R. W. *Macromolecules* **1996**, *29*, 3247.
(15) Cole, H. *J. Chem. Phys.* **1965**, *42*, 637.
(16) Nee, T. H.; Zwanzig, R. *J. Chem. Phys.* **1970**, *52*, 6353.
(17) Williams, G. *Chem. Soc. Rev.* **1977**, *7*, 89.
(18) Kohlrausch, R. *Prog. Ann. Phys.* **1854**, *91*, 179.
(19) Ishida, Y.; Yamafuji, K. *Kolloid-Z.* **1961**, *177*, 87.
(20) Zetsche, A.; Fischer, E. W. *Acta Polym.* **1994**, *45*, 168.

MA9712615